lubricants

MDPI

Article

Effects of Laser Surface Texturing and Lubrication on the Vibrational and Tribological Performance of Sliding Contact

Shunchu Liu [1], Qingyi Sai [2,*], Shuwen Wang [1,*] and John Williams [3]

[1] College of Mechanical Engineering, University of Shanghai for Science and Technology, Shanghai 200093, China; lsc9784@163.com
[2] College of Energy and Power Engineering, University of Shanghai for Science and Technology, Shanghai 200093, China
[3] Robinson College, University of Cambridge, Cambridge CB3 9AN, UK; jaw1000@cam.ac.uk
* Correspondence: saiqingyi@163.com (Q.S.); wsw@usst.edu.cn(S.W.)

Abstract: Various textures are fabricated by a picosecond laser machine on the surfaces of circular stainless steel specimens. Vibrational and tribological effects of laser surface textures are investigated by means of a tribometer and a data acquisition and signal processing (DASP) system. Experimental results show that surface textures can reduce the coefficients of friction (COFs), enhance the wear resistance, and improve the dynamical performance of frictional surfaces. In this study, the surface with micro circular dimples in diameter of 150 μm or textured area density of 25% has the best tribological and dynamical performance. Compared with the non-textured surface, the surface with circular dimples in diameter of 150 μm and 15% textured area density has 27% reduction of COFs, 95% reduction of frictional vibrations, and 66% reduction of frictional noise. The frictional vibrations and noise in the sliding contacts can be effectively reduced by adding graphene to the lubrication oil, and the surface textures enhance the frictional noise reduction performance of lubrication.

Keywords: laser surface texturing; noise; vibration; friction reduction; wear resistance; lubrication

Citation: Liu, S.; Sai, Q.; Wang, S.; Williams, J. Effects of Laser Surface Texturing and Lubrication on the Vibrational and Tribological Performance of Sliding Contact. *Lubricants* **2022**, *10*, 10. https://doi.org/10.3390/lubricants10010010

Received: 21 November 2021
Accepted: 5 January 2022
Published: 11 January 2022

1. Introduction

The phenomenon of friction and wear exists everywhere in the world, where there are surfaces in relative motion [1]. Although smoother surfaces can provide lower friction, recent studies show that rough surfaces with certain microstructures have better friction reduction, wear resistance, and lubrication performance [2–6]. In these studies, various techniques have been used to manufacture the surface micro structures, such as abrasive jet machining (AJM) [4], micro-electrical etching (MEE) [5], and laser surface texturing (LST) [6]. Since LST has the advantages of fast manufacturing and processing speed, no pollution to the environment, excellent shape and size control ability, this technology has attracted increasing attention in academic research and engineering applications.

Etsion et al. [6,7] are early representatives of the application research on LST. The authors used the laser micro modeling technology to process micro-pit arrays on the surface of piston rings. In addition, they studied the effect of depth, diameter, and area occupancy of the micro-structures on the tribological properties of functional surfaces. In the following decade, many studies used similar methods to experimentally study the effects of geometry, size, and density of surface texture and the contact mode of friction pair on the friction, wear, and lubrication properties of functional surfaces [8–26]. Various functional materials were used in these studies, including steels [8–16], cast iron [17–19], alloys [20–22], and compound materials [23,24], etc. The results of these experimental studies showed that LST had a positive effect on the reduction of friction and wear. However, some unsuccessful cases of using textures under high contact pressures of non-conformal contacts have been reviewed by Gachot et al. [25]. For instance, the reciprocating sliding tests of lubricated steel surfaces for a line contact under low contact pressures did not show positive effects of

surface texturing on friction [26], and the pin-on-disk tests (unidirectional sliding) under full film lubrication [27], although surface texturing slightly increased the film thickness [26] and expanded the operation range of loads and speeds for hydrodynamic lubrication [27].

More recently, bionic principles have been employed to the design of surface textures. Greiner et al. [28] used the laser processing technique to process the snake and lizard skin-like surface textures. The research results showed that LST reduced the sliding frictional forces by more than 40% under the condition of dry friction. Zheng et al. [29] used the method of laser heat treatment to carry out the bionic coupling of hardness gradient and hexagonal structure on the pre-engraved steel sample with an hexagonal surface structure. The results showed that the hexagonal texture processed by laser (HT-L) not only exhibited lower friction coefficient and less friction fluctuation than the similar surface hardness generated by conventional heat treatment but without hardness gradient (HT-H) and smooth surface treated by the same laser heat treatment as the HT-L (SS-L surfaces). In addition, the results demonstrated a substantial reduction of wear loss compared to the HT-H and SS-L surfaces.

In the last decade, investigation of the vibration and noise reduction performance of surface textures has become an interesting research area. Sudeep et al. [30] reported the friction and vibration behaviors of lubricated point contacts of reciprocating rolling motion on the surface with textures. In a combination of higher load and rolling speed, the surface textured contacts yielded significant reduction in rolling friction and vibration amplitude at resonant frequencies in comparison with the smooth contacts. The study of Meng et al. [31] showed that appropriately decreasing the eccentricity ratio or rotational speed can reduce the noise of the compound textured bearing. In addition, there is a critical length/diameter ratio of the bearing for suppressing the noise of the compound textured bearing. Wang et al. [32] studied the effects of diameter, depth, and area density of circular dimples on the friction, wear, and frictional noise of sliding contacts by 16 orthogonal designed experiments. Experimental results showed that laser surface textures can significantly reduce the friction and wear under rich oil lubrication, and reduce the frictional noise generated in steel-steel dry sliding contacts.

In the present study, three groups of parametric studies are carried out to experimentally investigate the effects of texture diameter, textured area density, and lubrication on the tribological performance of the textured surfaces. In addition, the effects of LST and lubrication on the reduction of frictional vibrations and noise are studied under oil-rich lubrication conditions. Moreover, the effects of lubricant with graphene particles on the tribological and dynamical performance of stainless steel surfaces without and with textures are investigated, and the softer upper specimens (aluminum alloy balls) are used.

2. Materials and Methods

2.1. Test Specimen Preparation

The commercial MDP31 picosecond laser processing system was used for the laser texturing, as shown in Figure 1a. The standard laser texturing process was followed in this study [33]. Figure 1b demonstrates the overview of the textures on the surface of the lower specimen, while Figure 1c–e illustrates the geometrical parameters of a single circular dimple. The specific laser processing parameters are shown in Table 1.

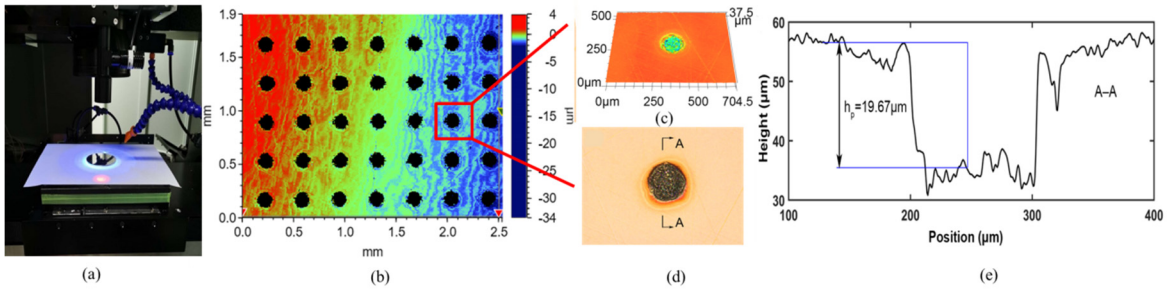

Figure 1. Laser processing system and processed textures on the surface of a lower specimen. (**a**) Laser processing system; (**b**) overview of the surface textures; (**c**) 3D of a texture; (**d**) 2D of a texture; (**e**) cross profile of a circular dimple.

Table 1. The technical parameters of laser processing system.

Parameter	Value	Unit
Laser wavelength	1064	nm
Laser output power	100	W
Acousto-optic modulation frequency	0.5~20	kHz
Maximum linear carving speed	3000	mm/s
Marking scope	45 × 45	mm
Repeated precision	2	μm
Positioning accuracy	2	μm
Marking line depth	0.001~0.1	mm

The tribo-pair consists of a lower specimen and an upper specimen. The lower specimen was a circular stainless-steel plate in diameter of 70 mm, and the upper specimen was a bearing-steel or aluminum alloy ball in diameter of 5 mm. The material properties of the lower and upper specimens are shown in Table 2. Seven lower specimens with circular dimples on their surfaces were manufactured by means of the laser machine shown in Figure 1a. The depths of all the circular dimples are the same (25 μm). However, the diameters and area densities of surface textures on these specimens are different, and are divided into three groups for the convenience of comparison. Table 3 shows the experimental arrangement and the dimensional parameters of the laser machined specimens in this study.

Table 2. The material properties of lower and upper specimens.

Materials	Type	Young's Modulus (GPa)	Hardness (HB)	Density (g/cm^3)
Steel plate	SUS304	193	205~210	7.93
Steel ball	GCr15	208	740~860	7.81
Al ball	5052	72	120~160	2.72

Table 3. Experimental arrangement.

Parametric Study	Texture Diameter (μm)	Textured Area Density (%)	Sliding Speed (m/s)	Upper Specimen
Effect of texture diameter	0	0	1.0	Bearing steel ball
	130	15	1.0	
	150	15	1.0	
	190	15	1.0	
Effect of textured area density	0	0	0.5	Bearing steel ball
	140	15	0.5	
	140	25	0.5	
	140	35	0.5	
Effect of lubricant	0	0	1.0	Aluminum alloy ball
	140	25	1.0	

2.2. Test Rig

In this experimental study, the UMT-TriboLab Mechanical Tester and Tribometer (manufactured by Bruker in the United States) was employed to investigate the tribological performance of the stainless-steel plate with surface textures. The loading force of the tribometer is in the range of 5~500 mN or 10~1000 N, the spindle speed is in the range of 0.1~5000 rpm, and the torque is up to 5 Nm. The accuracies of both the force and torque sensors are 0.02% of full-scale values. Figure 2a,b illustrates the experimental setup and the contact of the friction pair, respectively. The frictional vibrations were measured by a three-direction accelerometer (Kistler 8766A50M5) with a sampling rate of 51 kHz and processed by the data acquisition and signal processing (DASP) system developed by Beijing Oriental Institute of Vibrations and Noise (BOIVN), while the frictional noise was measured by means of a microphone (sound sensor INV3062W developed by BOIVN) with a sampling rate of 51 kHz, as shown in Figure 2a.

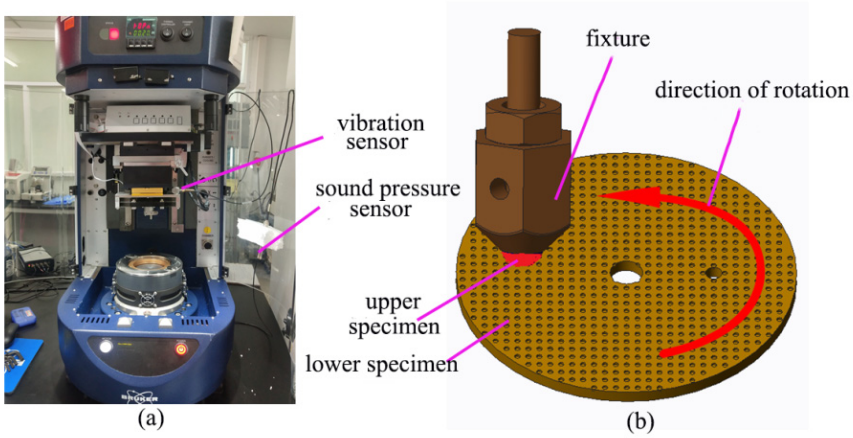

Figure 2. The UMT-TriboLab and experimental setup. (**a**) Tribometer; (**b**) illustration of sliding contact pair.

2.3. Experimental Methodology

In the tribological tests with the UMT-TriboLab, the upper specimen was a stationary bearing steel or aluminum alloy ball, and the lower specimen was a rotating stainless steel plate without or with surface textures, as shown in Figure 2b. Each experiment was repeated three times on the same lower specimen with the same normal contact force and relative sliding speed at different locations on the surface of the lower specimen. In addition, a new identical bearing steel ball or aluminum alloy ball (the upper specimen) was used for each repeated test. To investigate the effect of lubrication on the tribological and vibrational performance of surface textures, two different lubricants were used (A: Castrol

5W-30 engine oil and B: Castrol 5W-30 engine oil with 0.1% graphene added) and the identical aluminum alloy balls were used as upper specimens in these tests. The properties of lubricants A and B are shown in Table 4. The lubricants A and B and the graphene used in this study was provided by the Center of Green Lubrication, Chinese Academy of Sciences Shanghai Advanced Research Institute. The lateral size of the graphene sheet is about tens of microns, and the graphene sheet thickness is between 4 and 5 nm. The theoretical thickness of a single layer of graphene is about 0.34 nm, thus the number of graphene layers is about 10, and the average size of graphene particles is about 16.2 μm in diameter. More details regarding the characteristics of the graphene used in this study can be found in [34].

Table 4. The properties of lubricating oil.

Types of Lubricants	Characteristic	Value	Unit	Test Standard
Lubricant A (Castrol 5w-30)	Density (ρ1 /15.6 °C)	849	kg/m^3	ASTM D4052
	Viscosity (η1/100 °C)	0.009594	Pa·s	ASTM D445
	Flash point	230	°C	ASTM D92
	Total base number	11.3	TBN	ASTM D2896
Lubricant B (Castrol 5W-30 with 0.1% graphene added)	Density (ρ2 /15.6 °C)	860	kg/m^3	ASTM D4052
	Viscosity (η2/100 °C)	0.009718	Pa·s	ASTM D445
	Flash point	>200	°C	ASTM D92
	Total base number	11.3	TBN	ASTM D2896

Above the upper specimen, a force sensor and a torque sensor were fixed on the tribometer, which were used to measure the normal contact force and frictional force of the sliding contact during tests, respectively. The coefficients of friction (COFs) were obtained via the built-in data acquisition system of the tribometer. During the tests, the lower specimen (stainless steel plate) was fully covered by the lubrication oil. The tests were carried out at room temperature, and each experiment lasted for the same contact distance of 100 m under the same normal load of 10 N. After the tests, the specimens were ultrasonically cleaned and the wear losses (wear depths and volumes) of both the upper and lower specimens were measured using a white light interference profilometer, the Bruker ContourGT-K 3D Optical Microscope.

3. Experimental Results and Discussion

3.1. Effect of LST on COFs

3.1.1. Texture Diameter

Figure 3a demonstrates the effect of texture diameter on the measured COFs of bearing steel ball sliding, which is contacted with a stainless steel plate with 15% textured area density at a sliding speed of 1 m/s. In Figure 3a, it can be seen that the COFs are significantly reduced by the surface textures in all of the tests, although they are not so significant in the first 5 s of the tests. This is due to the fact that in the first few seconds the sliding contacts are in the transit states. Moreover, Figure 3a shows that the circular dimples in diameter of 150 μm have the best performance in friction reduction, 27% less than the specimens without a surface dimple, while the specimen with circular dimples in diameter of 130 μm has the similar performance in friction reduction with the specimen with circular dimples in diameter of 190 μm, about 10% less than the specimen without a surface texture.

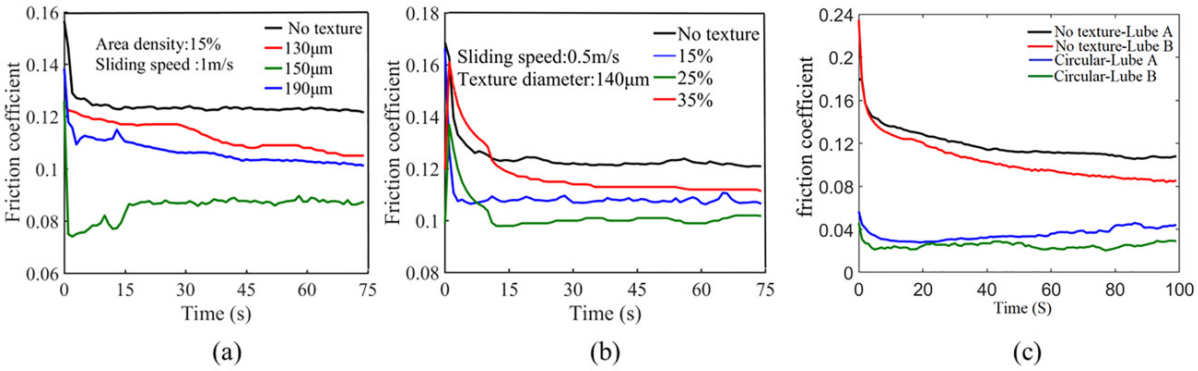

Figure 3. Effect of surface textures and lubrication on COFs. (**a**) Circular dimple diameter; (**b**) textured area density; (**c**) lubrication.

3.1.2. Area Density

Figure 3b shows the effect of textured area density on the COFs of bearing steel ball sliding which is contacted on a stainless steel plate with surface textures in diameter of 140 μm at sliding speed of 0.5 m/s. In Figure 3b, it can be seen that the specimen surface with 25% textured area density has a 20% reduction on the COFs, while an 8% reduction of the COFs is obtained when the textured area density is 35%. The effect of 15% textured area density on the friction reduction is in the middle of the three studied textured area densities.

3.1.3. Lubricant

Figure 3c presents the friction coefficients of textured and non-textured surfaces under two different lubricants, lubricant A and lubricant B. In these studies, aluminum alloy balls were used as upper specimens, and circular stainless steel plates with surface textures in diameter of 140 μm and 25% textured area density were used as lower specimens, at the sliding speed of 1 m/s and normal load of 10 N.

In Figure 3c, it can be seen that under the same lubricant the COFs of the textured surface are significantly less than the non-textured surface. In addition, the COFs from the sliding contacts of non-textured surface and aluminum alloy balls are decreasing in the whole period of testing. However, on the textured surfaces, the COFs are decreasing only in the first 5 s and then become stable.

Moreover, Figure 3c shows that the COFs of both the textured and smooth surfaces are reduced by adding graphene to the lubrication oil. This is due to the fact that graphene has an ultra-thin layered structure, which is easy to adhere to the frictional contact surfaces and reduce the direct contact between the friction counterparts [35–37].

3.2. Effect of LST on Wear

3.2.1. Texture Diameter

In this study, a white light interference profilometer, the Bruker ContourGT-K 3D optical microscope was employed to measure the wear losses (volume) of the tested specimens. Figure 4a,b demonstrates the surface topographies of the upper and lower specimens without and with surface textures in area density of 15% and diameter of 130 μm, after sliding friction tests under the same operation conditions of normal load 10 N and sliding speed 1 m/s. Figure 4a,b shows that the wear volume of the textured surface is considerably smaller than the non-textured surface. The wear scar of the non-textured surface is about 10.43 μm in depth and 1200 μm in width, while the wear scar on the surface with textures in diameter of 130 μm is only about 3.2 μm in depth and 70 μm in width. In Figure 4a,b, it can be seen that the wear volume of the steel ball which is contacted with the textured surface is considerably smaller than the steel ball which is contacted with the untextured surface.

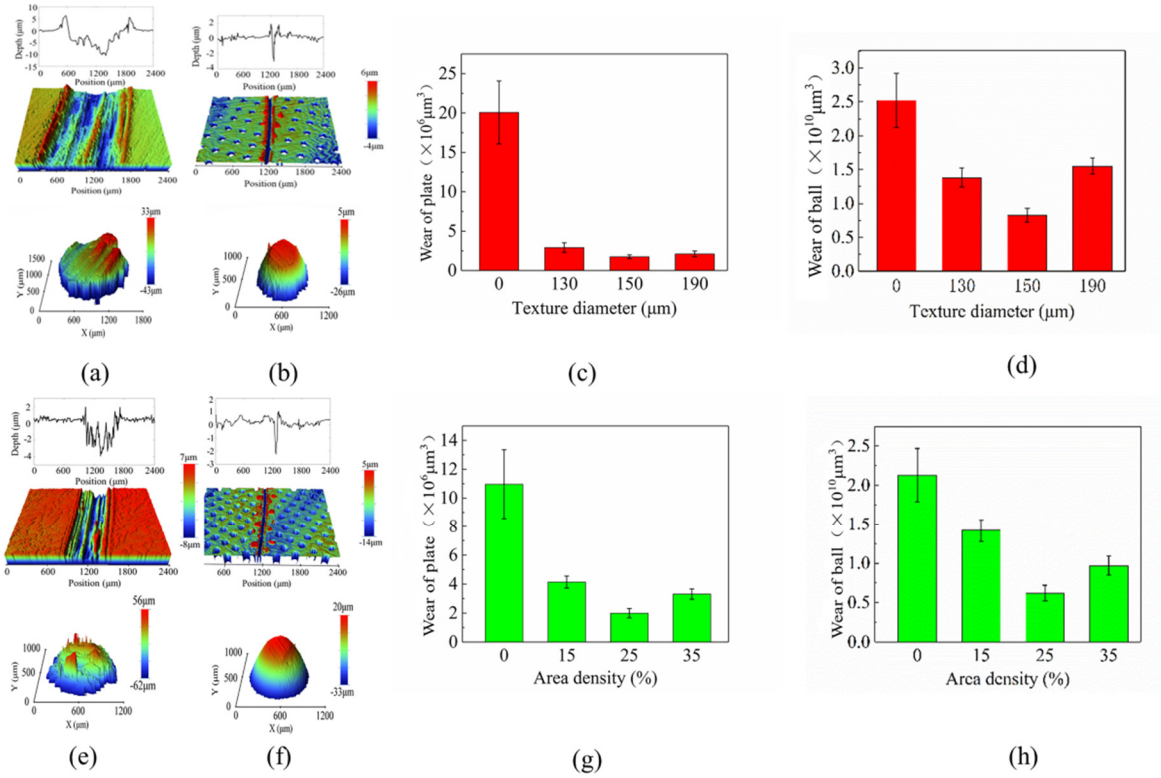

Figure 4. Surface topographies and wear of lower and upper specimens after tests under 10 N of normal load. (**a**) Surface topographies of upper and lower specimens without a surface texture after sliding tests; (**b**) surface topographies of upper and lower specimens with surface textures in diameter of 130 μm after sliding tests; (**c**) the effect of texture diameter on the wear of lower specimen; (**d**) the effect of texture diameter on the wear of upper specimen; (**e**) surface topographies of upper and lower specimens without a surface texture after sliding tests; (**f**) surface topographies of upper and lower specimens with surface textures in diameter of 140 μm and area density of 25% after sliding tests; (**g**) the effect of textured area density on the wear of lower specimen; (**h**) the effect of textured area density on the wear of upper specimen.

Figure 4c,d presents the effect of texture diameter on the wear volume of lower and upper specimens, respectively. Figure 4c shows the wear volume of a specimen without a surface texture and three textured specimens with circular dimples in diameters of 130, 150, and 190 μm at the same sliding speed of 1 m/s and normal load of 10 N. In Figure 4c, it can be seen that the wear volume of the specimen without a surface texture is almost 10 times the specimen with a surface texture. The wear volume of the textured specimen with surface circular dimples in diameter of 150 μm is less than the specimen with 130 and 190 μm in diameter of circular dimples.

Figure 4d shows the wear volume of the upper specimen (bearing steel balls) against the specimens without a texture and with circular dimples in diameters of 130, 150, and 190 μm at the same sliding speed of 1 m/s and normal load of 10 N. In Figure 4d, it can be seen that the wear volume of the steel ball against the specimen without a texture is about twice the amount of steel balls against the textured specimens. The wear volume of the steel ball against the textured specimens with surface circular dimples in diameter of 150 μm is less than the two specimens with circular dimples in diameters of 130 and 190 μm.

3.2.2. Area Density

Similarly, Figure 4e,f shows the surface topographies of the upper and lower specimens without a surface texture and with circular dimples in diameter of 140 μm and 25% textured

area density, respectively, after lubricated non-conformal sliding contacts. Figure 4e shows that the wear scar on the non-textured specimen surface is about 3.93 μm in depth and 900 μm in width, while in Figure 4f, the wear scar on the specimen with 25% textured area density is only about 2.24 μm in depth and 75 μm in width. Figure 4e,f also shows the topographies of the upper specimen after sliding which is contacted with the lower specimen without and with surface textures, respectively. In Figure 4e, the wear of the upper specimen (steel ball) is significantly larger than the wear shown in Figure 4f.

Figure 4g demonstrates the effect of textured area density on the wear of the lower specimen of stainless steel plate. In Figure 4g, it can be seen that the surface textured area density has a significant effect on the wear of the contact surface. The surface with a textured area density of 25% has the smallest wear off compared with the surfaces with textured area densities of 15% and 35%.

Figure 4h demonstrates the effect of textured area density of the lower specimen on the wear of the upper specimen (bearing steel ball). In Figure 4h, it can be seen that the surface textured area density of the lower specimen has a significant effect on the wear of the upper specimen. When the lower specimen has a 25% textured area density, the upper specimen (bearing steel ball) has the smallest wear compared with the area density against the lower specimens with textured area densities of 15% and 35%.

3.2.3. Lubricant

Figure 5 shows the wear of the upper specimen (Al ball) in contact with the textured and non-textured surfaces lubricated with lubricant A and lubricant B. In Figure 5, it can be seen that when the normal contact force is the same and under the same lubricant, the wear of the upper specimen (Al ball) in contact with the textured specimen is significantly less than when it is in contact with the non-textured surface. Moreover, the wear of the upper specimen (Al ball) is significantly reduced by adding 0.1% of graphene to the lubricant for both the textured and non-textured surfaces.

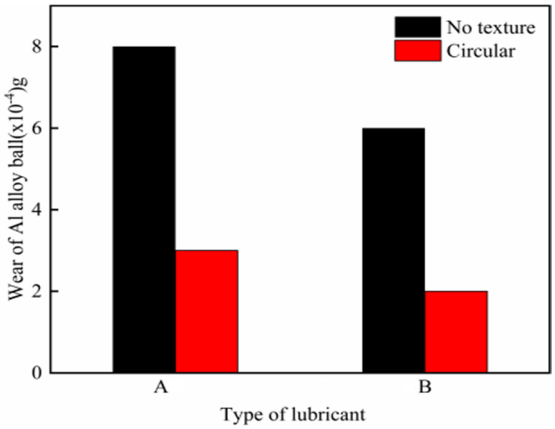

Figure 5. Effect of lubrication on the wear of aluminum alloy ball.

3.2.4. The Mechanism of Friction and Wear Reduction by LST

Based on the tribological studies in the present and previous studies, the mechanism of the positive effect of LST on the friction and wear reduction can be summarized in general. First, the existence of surface textures changes the lubrication condition on the frictional surfaces. In the starved lubrication condition, textures store lubricants and improve the surface lubrication performance. In the oil-rich lubrication condition, textures have an hydrodynamic lubrication (HL) or Elasto-hydrodynamic lubrication (EHL) effect and improve the bearing performance of the lubricated surface. Second, surface textures reduce the friction contact area, store the abrasive particles, and prevent the wear caused by the third body (abrasive particles) between the frictional contact surfaces. Third, laser surface texturing (LST) increases the surface hardness and decreases the tensile residual

stress [38] or increases the compressive residual stress of the laser textured surface [39]. Therefore, improving the wear resistance of the textured surface.

The effects of circular dimple diameter, textured area density or lubricants on the friction and wear performance of the textured surfaces can be summarized based on the previous studies. Mohmad et al. [40] pointed out that textures can only function well at a certain range of diameter size. Smaller diameters have difficulty in generating the hydrodynamic loading capacity, while larger diameters may increase the roughness of contact surfaces and increase the coefficients of friction.

Li et al. [23] reported that the dimples on the surface with a lower textured area density were not sufficient for storing lubricants and had difficulty in generating the hydrodynamic loading capacity. In contrast, with an increase of the dimple density, the number of dimple increases and the surface roughness increases significantly, which reduces the wear life of oil film. A texture with moderate dimple density provides sufficient lubricant storage, and its relatively lower roughness is beneficial to the wear life of oil film.

In the present study, graphene was added to lubricant-B. in addition, the research of Sarno et al. [36] showed that the graphene platelets in oil easily form a protective film to prevent the direct contact between two contact surfaces, Therefore, this improves the frictional behavior of the lubricant.

3.3. Effect of LST on Frictional Vibrations

3.3.1. Texture Diameter

Figure 6a–d shows the frictional vibrations of surfaces without and with textures in area density of 25% and diameters of 130, 150, and 190 μm in frequency domain, respectively. In Figure 6a–d, it can be seen that the surface textures have a significant effect on the reduction of frictional vibrations. In addition, the circular dimples in diameter of 150 μm have the best performance in the reduction of frictional vibrations. Moreover, Figure 6b,d shows that the frictional vibrations significantly reduced after 40 s of sliding contacts. However, for the smooth surface, the frictional vibrations increased after 40 s of sliding contacts, which is possibly due to the more serious wear of the surface without laser texturing, as shown in Figure 6a.

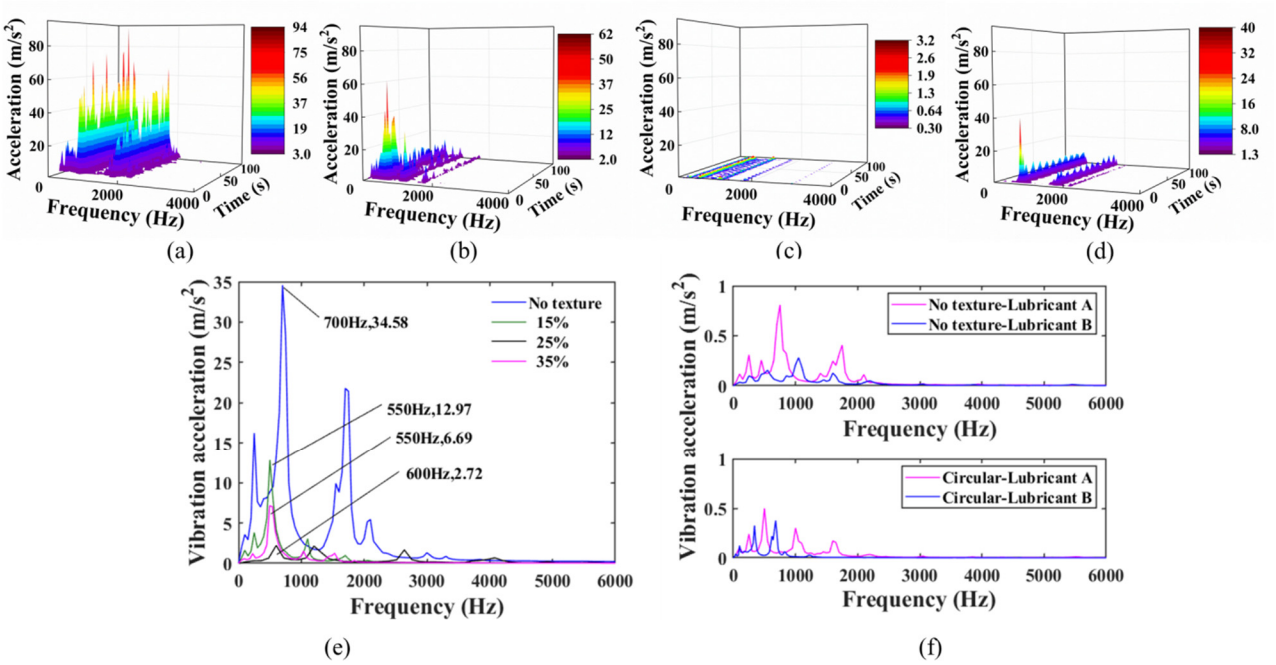

Figure 6. Effect of surface texture diameter, textured area density, and lubrication on frictional vibrations. (**a**) No texture; (**b**) 130 μm in diameter; (**c**) 150 μm in diameter; (**d**) 190 μm in diameter; (**e**) effect of area density; (**f**) effect of lubrication and texture.

Table 5 lists the RMSs of measured vibrations in time domain, the vibration reduction rate compared with the non-textured specimen under the same working conditions, the main resonant frequency of vibrations, and the peak resonant vibration amplitudes. In Table 5, it can be seen that under the normal load of 10 N at sliding speed of 1 m/s with textured area density of 15%, the measured frictional vibrations from the surface with circular dimples in diameter of 150 μm are reduced to about 5% of the vibrations induced by the surface without a surface texture in time domain, which has a better performance in vibration reduction than the specimens with surface circular dimples in diameters of 130 and 190 μm.

Table 5. RMS of normal vibrations generated from sliding contacts in time domain.

Test			RMS (Time Domain) (m/s^2)	Vibration Reduction (%)	Peak Resonant Frequency/ Amplitude
Diameter (μm)	Area Density (%)	Speed (m/s)		Time Domain	
0	0	1	49.6311	/	700 Hz, 34.58
130	15	1	16.2964	67.2	550 Hz, 12.34
150	15	1	2.4190	95.1	500 Hz, 1.82
190	15	1	10.3100	79.2	750 Hz, 7.94
0	0	0.5	29.6885	/	1700 Hz,17.86
140	15	0.5	16.2964	45.1	500 Hz, 12.97
140	25	0.5	3.6681	87.6	600 Hz, 2.72
140	35	0.5	7.5730	74.5	550 Hz, 6.69

3.3.2. Area Density

Similarly, it can be seen from Figure 6e that the surface with textures in diameter of 140 μm and 25% textured area density has a better performance in vibration reduction than the 15% and 35% textured area densities. In Figure 6e, it can be seen that the peak resonance frequency of the frictional vibrations generated from the non-textured surface is 700 Hz. However, the peak resonant frequency of the frictional vibrations generated from the textured surfaces is changed to 550 and 600 Hz. The decrease of the peak resonant frequency may be due to the decrease in the contact stiffness caused by surface texturing. In addition, the reduction of frictional vibrations in amplitude at resonance may be attributed to the increased damping due to the surface dimple squeezing film effect [41].

Moreover, in Table 5, it can be seen that under the same sliding speed and texture diameter, the measured RMS vibration amplitudes from the specimen with 25% textured area density are reduced more than 87% in time domain, which have the best performance in vibration reduction among the three specimens with different textured area densities.

3.3.3. Lubricant

Figure 6f presents the measured frictional vibrations in frequency domain from the Al alloy ball sliding contacts with the textured and un-textured lower specimen under two different lubrications. In these experiments, two different lubricants, A and B, were used under the experimental conditions of sliding speed of 1 m/s, normal load of 10 N, and the textured area density of 25%. In Figure 6f, it can be seen that both the surface texture and lubrication have a significant effect on the frictional vibrations. Moreover, Figure 6f shows that the peak vibration amplitude generated from the non-textured surface with lubricant B is 44% lower than the amplitude generated from the non-textured surface with lubricant A, while the peak vibration amplitude from the textured surface with lubricant B is 14% lower than the amplitude generated with lubricant A. Graphene as an additive of lubricants can effectively reduce the frictional vibrations on both textured and non-textured surfaces. However, the effect of lubrication on the reduction of frictional vibrations is reduced by surface textures.

3.4. Effect of LST on Frictional Noise

3.4.1. Texture Diameter

The frictional noise measured during the tribological tests with a sound pressure sensor is shown in Figure 7. Figure 7a–d shows that the diameters of surface textures have a significant effect on the reduction of frictional noise, and the 150 μm in diameter circular dimples have better performance in the reduction of frictional noise than the textures in diameters of 130 and 190 μm.

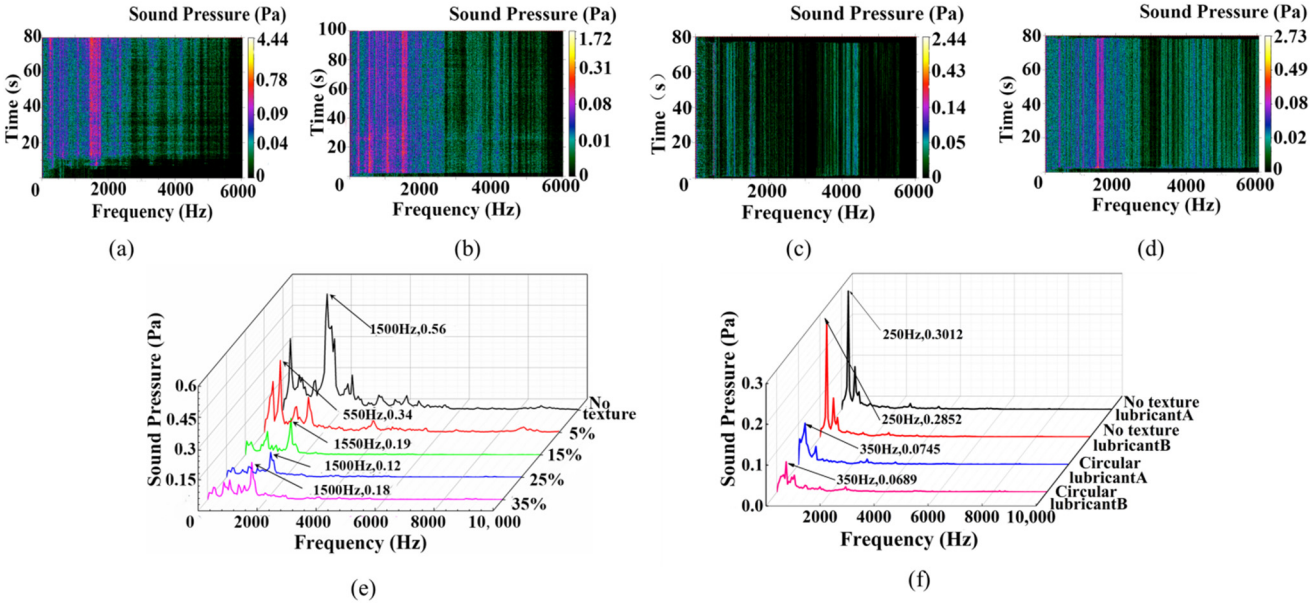

Figure 7. Effect of surface dimple diameter, textured area density, and lubrication on frictional noise. (**a**) No texture; (**b**) 130 μm; (**c**) 150 μm; (**d**) 190 μm; (**e**) effect of area density with bearing steel ball; (**f**) effect of lubrication and surface texture with aluminum alloy ball.

Table 6 lists the RMSs of measured frictional noise in time domain, the noise reduction rate in time domain, the main resonant frequency of frictional noise, and the noise amplitude at peak resonant frequency. In Table 6, it can be seen that the frictional noise from the textured specimen is considerably lower than the non-textured specimen under the same experimental conditions. In addition, the RMS of frictional noise from the textured surface with 150 μm in diameter dimples has 66% reduction in time domain compared with the RMS from the non-texture specimen under the same working conditions.

Table 6. RMS and reduction rate of frictional noise generated from sliding contacts in time domain.

Test		RMS (Time Domain) (m/s^2)	Noise Reduction (%)	Resonant Frequency/ Amplitude
Diameter (μm)	Area Density (%)		Time Domain	
0	0	1.0085	/	1500 Hz, 0.56
130	15	0.4870	52	1500 Hz, 0.24
150	15	0.344	66	500 Hz, 1.82
190	15	0.8524	15	750 Hz, 7.94
140	5	0.6768	33	550 Hz, 0.34
140	15	0.3124	69	1550 Hz, 0.19
140	25	0.2707	73	1500 Hz, 0.12
140	35	0.3169	68	1500 Hz, 0.18

3.4.2. Area Density

Figure 7e shows that the surface with 25% textured area density has better performance in noise reduction than the 15% and 35% textured area densities, as the circular dimple diameter is 140 μm. In Table 6, it can be seen that the surface texture can significantly reduce the amplitude of frictional noise, and the surface with the textured area density of 25% has the most significant effect on the frictional noise reduction. Compared with the non-textured surface, 73% of the RMS of frictional noise in time domain generated by the textured surface (25% textured area density) is reduced. In addition, it is observed that the surface texture changes the peak resonant frequency of frictional noise.

3.4.3. Lubricant

Figure 7f presents the measured frictional noise in frequency domain from the Al alloy ball sliding contacts with the textured and untextured lower specimen under two different lubrications. In these experiments, two different lubricants were used under the experimental conditions of sliding speed of 1 m/s, normal load of 10 N, and the textured area density of 25%.

In Figure 7f, it can be seen that both the surface texture and lubrication have a significant effect on the frictional noise. Figure 7f shows that the peak sound pressure amplitude generated from the non-textured surface with lubricant B is 5% lower than the non-textured surface with lubricant A, while the peak sound pressure amplitude from the textured surface with lubricant B is 8% lower than lubricant A. Therefore, graphene as an additive of lubricants can effectively reduce the frictional noise on both the textured and non-textured surfaces. Figure 7f demonstrates that surface textures (circular dimples) have a more significant effect on the frictional noise reduction than the lubricants, and surface textures enhance the noise reduction performance of lubrication.

3.4.4. The Mechanism of Frictional Vibration and Noise Reduction by LST

From the dynamic tests in this study, it can be seen that LST has a significant effect on the reduction of frictional vibrations and noise. The mechanism of frictional vibration and noise reduction by LST can be summarized. Since the frictional noise and vibrations are excited by frictional forces that are proportional to the COFs of the frictional system, the frictional vibrations and noise can be reduced by surface textures due to the reduction of COFs. In addition, the LST reduces the wear on the contact surfaces, which has a significant effect on the reduction of frictional vibrations and noise. Moreover, LST reduces the tensile residual stress of the textured surface [38], which has a positive effect on the reduction of frictional vibrations and noise. Furthermore, laser surface texturing facilitated better lubrication on the contact surfaces, resulting in the improved contact stiffness and damping [41], which is beneficial to the reduction of frictional noise and vibrations.

4. Conclusions

Experimental studies have been carried out to investigate the effects of LST and lubrication with graphene on the tribological and dynamical performance of non-conformal sliding contacts. Significant friction/wear and frictional vibrations and noise reductions are observed in this study, and the following conclusions can be drawn:

(1) Under the operation conditions in this study, the circular dimples in diameter of 150 μm have a better tribological performance than those of 130 and 190 μm, while a textured area density of 25% has a better tribological performance than those with 15% and 35% textured area densities.

(2) Laser surface textures have a significant effect on the reduction of frictional vibrations and noise generated from steel-steel lubricated non-conformal sliding contacts in both the time and frequency domains. In this study, the maximum RMS reduction of frictional vibrations and noise is more than 95% and 70%, respectively, in the time and frequency domains.

(3) Adding graphene to the Castrol 5W-30 fully synthetic engine oil can improve the tribological and dynamical performance of lubrication. Surface textures (circular dimples) have a more significant effect on the frictional noise and vibration reduction than the lubricants, and surface textures enhance the frictional noise reduction performance of lubrication.

(4) When the upper specimen is an aluminum alloy ball, the effect of texture on the reduction of friction, vibration, and noise is more significant than the bearing steel ball upper specimen, which may be due to the more significant hydrodynamic effect generated by the surface textures sliding contact with the aluminum alloy balls. However, the mechanisms are required for further investigation.

Author Contributions: Conceptualization, S.W. and Q.S.; methodology, Q.S., S.W. and J.W.; validation, S.W. and S.L.; formal analysis, S.L. and S.W.; investigation, S.W. and S.L.; data curation, S.W. and S.L.; writing—original draft preparation, S.L. and Q.S.; writing—review and editing, S.W. and J.W.; supervision, S.W. and Q.S. All authors have read and agreed to the published version of the manuscript.

Funding: This research was financially supported by the Science and Technology Commission of Shanghai Municipality (grant number: 18060502400) and Natural Science Foundation of Shanghai (grant number: 21ZR1445000).

Data Availability Statement: The data presented in this study are available on request from the corresponding authors.

Conflicts of Interest: The authors declare no conflict of interest.

References

1. Chen, K.Y.; Yang, X.F.; Zhang, Y.F.; Yang, H.; Lv, G.J.; Gao, Y.L. Research progress of improving surface friction properties by surface texture technology. *Int. J. Adv. Manuf. Technol.* **2021**, *116*, 1797–2821. [CrossRef]
2. Shinkarenko, A.; Kligerm, Y.; Etsion, I. The effect of surface texturing in soft elasto-hydrodynamic lubrication. *Tribol. Int.* **2009**, *42*, 284–292. [CrossRef]
3. Pettersson, U.; Jacobson, S. Influence of surface texture on boundary lubricated sliding contacts. *Tribol. Int.* **2003**, *36*, 857–864. [CrossRef]
4. Uehara, Y.; Wakuda, M.; Yamauchi, Y.; Kanzaki, S.; Sakaguchi, S. Tribological properties of dimpled silicon nitride under oil lubrication. *J. Eur. Ceram. Soc.* **2004**, *24*, 369–373. [CrossRef]
5. Yan, D.S.; Qu, N.S.; Li, H.S.; Wang, X.L. Significance of dimple parameters on the friction of sliding surfaces investigated by orthogonal experiments. *Tribol. Trans.* **2010**, *53*, 703–712. [CrossRef]
6. Etsion, I.; Sher, E. Improving fuel efficiency with laser surface textured piston rings. *Tribol. Int.* **2009**, *42*, 542–547. [CrossRef]
7. Ryk, G.; Etsion, I. Testing piston rings with partial laser surface texturing for friction reduction. *Wear* **2006**, *261*, 792–796. [CrossRef]
8. Elo, R.; Heinrichs, J.; Jacobson, S. Surface texturing to promote formation of protective tribofilms on combustion engine valves. *Proc. Inst. Mech. Eng. Part J* **2018**, *232*, 54–61. [CrossRef]
9. Wang, L.L.; Guo, S.H.; Wei, Y.L.; Yuan, G.T. Research on the influence of micropits structure on the tribological performance of friction pairs. *Proc. Inst. Mech. Eng. Part J* **2019**, *233*, 317–325. [CrossRef]
10. Andersson, P.; Koskinen, J.; Varjus, S.; Gerbig, Y.; Haefke, H.; Gergiou, S.; Zhmud, B.; Buss, W. Microlubrication effect by laser-textured steel surfaces. *Wear* **2007**, *262*, 369–379. [CrossRef]
11. Tang, W.; Zhou, Y.K.; Zhu, H.; Yang, H.F. The effect of surface texturing on reducing the friction and wear of steel under lubricated sliding contact. *Appl. Surf. Sci.* **2013**, *273*, 199–204. [CrossRef]
12. Rapoport, L.; Moshkovich, A.; Perfilyev, V.; Gedanken, A.; Koltypin, Y.; Sominski, E.; Halperin, G.; Etsion, I. Wear life and adhesion of solid lubricant films on laser-textured steel surfaces. *Wear* **2009**, *267*, 1203–1207. [CrossRef]
13. Sudeep, U.; Pandey, R.K.; Tandon, N. Effects of surface texturing on friction and vibration behaviors of sliding lubricated concentrated point contacts under linear reciprocating motion. *Tribol. Int.* **2013**, *62*, 198–207. [CrossRef]
14. Segu, D.; Kim, S. Influence on friction behavior of micro-texturing under lubricated non-conformal contact. *Meccanica* **2014**, *49*, 483–492. [CrossRef]
15. Duffet, G.; Sallamand, P.; Vannes, A. Improvement in friction by cw Nd:YAG laser surface treatment on cast iron cylinder bore. *Appl. Surf. Sci.* **2002**, *205*, 289–296. [CrossRef]
16. Lu, P.; Wood, R.J.K.; Gee, M.G.; Wang, L.; Pfleging, W. A novel surface texture shape for directional friction control. *Tribol. Lett.* **2018**, *66*, 51. [CrossRef]
17. Saeidi, F.; Meylan, B.; Hoffmann, P.; Wasmer, K. Effect of surface texturing on cast iron reciprocating against steel under starved lubrication conditions: A parametric study. *Wear* **2016**, *348*, 17–26. [CrossRef]

18. Nakano, M.; Korenaga, A.; Korenaga, A.; Miyake, K.; Murakami, T.; Ando, Y.; Usami, H.; Sasaki, S. Applying micro-texture to cast iron surfaces to reduce the friction coefficient under lubricated conditions. *Tribol. Lett.* **2007**, *28*, 131–137. [CrossRef]
19. Kumar, B.; Babu, P.; Marimuthu, P. Effect of laser surface texturing on tribological behaviour of grey cast iron. *Int. J. Surf. Sci. Eng.* **2019**, *13*, 220–235. [CrossRef]
20. Vasumathy, D.; Meena, A. Influence of micro scale textured tools on tribological properties at tool-chip interface in turning AISI 316 austenitic stainless steel. *Wear* **2017**, *376*, 1747–1758. [CrossRef]
21. Sun, Q.C.; Hu, T.C.; Fan, H.Z.; Zhang, Y.S.; Hu, L.T. Dry sliding wear behavior of TC11 alloy at 500 °C: Influence of laser surface texturing. *Tribol. Int.* **2015**, *92*, 136–145. [CrossRef]
22. Kovalchenko, A.; Ajayi, O.; Erdemir, A.; Fenske, G. Friction and wear behavior of laser textured surface under lubricated initial point contact. *Wear* **2010**, *271*, 1719–1725. [CrossRef]
23. Li, J.L.; Xiong, D.S.; Dai, J.H.; Huang, Z.J.; Tyagi, R. Effect of surface laser texture on friction properties of nickel-based composite. *Tribol. Int.* **2009**, *43*, 1193–1199. [CrossRef]
24. Borghi, A.; Gualtieri, E.; Marchetto, D.; Moretti, L.; Valeri, S. Tribological effects of surface texturing on nitriding steel for high-performance engine applications. *Wear* **2008**, *265*, 1046–1051. [CrossRef]
25. Gachot, C.; Rosenkranz, A.; Hsu, S.M.; Costa, H.L. A critical assessment of surface texturing for friction and wear improvement. *Wear* **2017**, *372*, 21–41. [CrossRef]
26. Costa, H.L.; Hutchings, I.M. Hydrodynamic lubrication of textured steel surfaces under reciprocating sliding conditions. *Tribol. Int.* **2007**, *40*, 1227–1238. [CrossRef]
27. Kovalchenko, A.; Ajayi, O.; Erdemir, A.; Fenske, G.; Etsion, I. The effect of laser surface texturing on transitions in lubrication regimes during unidirectional sliding contact. *Tribol. Int.* **2005**, *38*, 219–225. [CrossRef]
28. Greiner, C.; Schäfer, M. Bio-inspired scale-like surface textures and their tribological properties. *Bioinspir. Biomim.* **2015**, *10*, 044001. [CrossRef]
29. Zheng, L.; Wu, J.J.; Sun, S.S.; Zhang, Z.H.; Liang, S.; Liu, Z.N.; Ren, L.Q. Bionic coupling of hardness gradient to surface texture for improved anti-wear properties. *J. Bionic Eng.* **2016**, *13*, 406–415. [CrossRef]
30. Sudeep, U.; Tandon, N.; Pandey, R. Friction and vibration behaviors of lubricated laser textured point contacts under reciprocating rolling motion with highlights on the used laser parameters. *Procedia Technol.* **2014**, *14*, 4–11. [CrossRef]
31. Meng, F.; Shu, R.; Chen, L. Influences of operation parameters on noise of journal bearing with compound texture considering lubricant thermal effect. *Proc. Inst. Mech. Eng. Part J* **2020**, *234*, 991–1006. [CrossRef]
32. Wang, S.W.; Chen, A.; Li, L.; Zhang, X.G. Tribological and vibrational effects of laser surface texturing on steel-steel sliding contact. *J. Phys. Conf. Ser.* **2018**, *1106*, 11. [CrossRef]
33. Schreck, S.; Gahr, K. Laser-assisted structuring of ceramic and steel surfaces for improving tribological properties. *Appl. Surf. Sci.* **2005**, *247*, 616–622. [CrossRef]
34. Kong, S.; Hu, W.J.; Li, J.S. Tribological properties of graphene in PAO base oil. *China Surf. Eng.* **2019**, *32*, 162–169.
35. Yang, H.M.; Li, J.S.; Zeng, X.Q. Tribological behavior of alkylamine edge functionalized graphene oxide pickering emulsion. *China Surf. Eng.* **2019**, *32*, 151–159.
36. Sarno, M.; Senatore, A.; Cirillo, C.; Petrone, V.; Ciambell, P. Oil lubricant tribological behaviour improvement through dispersion of few layer grapheme oxides. *J. Nanosci. Nanotechnol.* **2014**, *14*, 4960–4968. [CrossRef]
37. Bhaumik, S.; Kamaraj, M.; Paleu, V. Tribological analyses of a new optimized gearbox biodegradable lubricant blended with reduced graphene oxide nanoparticles. *Proc. Inst. Mech. Eng. Part J* **2021**, *235*, 901–915. [CrossRef]
38. Wang, S.W.; Guo, W.; Zeng, K.; Zhang, X.G. Characterization of automotive brake discs with laser-machined surfaces. *Automot. Innov.* **2019**, *2*, 190–200. [CrossRef]
39. Wang, S.W.; Yan, F.Y.; Chen, A. Tribological effects of laser surface texturing and residual stress. *Ind. Lubr. Tribol.* **2018**, *70*, 126–132. [CrossRef]
40. Mohmad, M.; Abdollah, M.; Tamaldin, N.; Amiruddin, H. The effect of dimple size on the tribological performances of a laser surface textured palm kernel activated carbon-epoxy composite. *Ind. Lubr. Tribol.* **2017**, *69*, 768–774. [CrossRef]
41. Sudeep, U.; Tandon, N.; Pandey, R.K. Vibration studies of lubricated textured point contacts of bearing steels due to surface topographies: Simulations and experiments. *Tribol. Int.* **2016**, *102*, 265–274. [CrossRef]